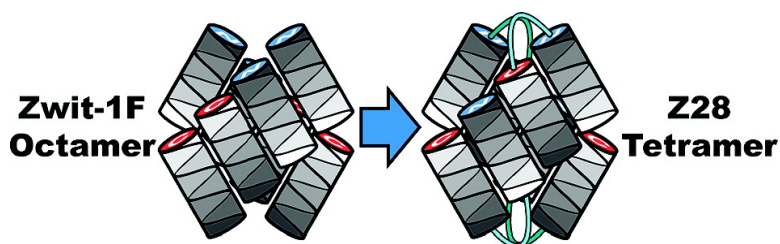


## Toward $\beta$ -Amino Acid Proteins: Design, Synthesis, and Characterization of a Fifteen Kilodalton $\beta$ -Peptide Tetramer

E. James Petersson, and Alanna Schepartz

*J. Am. Chem. Soc.*, **2008**, 130 (3), 821-823 • DOI: 10.1021/ja077245x

Downloaded from <http://pubs.acs.org> on February 8, 2009



### More About This Article

Additional resources and features associated with this article are available within the HTML version:

- Supporting Information
- Links to the 6 articles that cite this article, as of the time of this article download
- Access to high resolution figures
- Links to articles and content related to this article
- Copyright permission to reproduce figures and/or text from this article

[View the Full Text HTML](#)

## Toward $\beta$ -Amino Acid Proteins: Design, Synthesis, and Characterization of a Fifteen Kilodalton $\beta$ -Peptide Tetramer

E. James Petersson<sup>†</sup> and Alanna Schepartz<sup>\*,†,‡</sup>

Departments of Chemistry and Molecular, Cellular and Developmental Biology, Yale University,  
New Haven, Connecticut 06520-8107

Received September 18, 2007; E-mail: alanna.schepartz@yale.edu

Natural proteins are composed of linear chains of  $\alpha$ -amino acid monomers that adopt complex folded structures stabilized primarily by noncovalent interactions.<sup>1</sup> Within a single polypeptide chain, local interactions generate helix or sheet secondary structures and longer-range interactions generate tertiary structures—assemblies of multiple secondary structures.<sup>2</sup> Furthermore, multiple discrete polypeptides can associate to form quaternary complexes. This higher order structure is nearly universally responsible for the sophistication of protein function. Non-natural polymers have the potential for structural complexity and sophisticated function, but the design of such molecules is even more challenging than protein design because there exist no natural templates to mimic.<sup>3,4</sup>

Our efforts to design higher order  $\beta$ -peptide folds began with the synthesis of the oppositely charged  $\beta$ -peptides Acid-1F and Base-1F, which assemble in aqueous buffer into a stable, octameric quaternary complex.<sup>5</sup> To more fully characterize the structure and thermodynamics of Acid-1F/Base-1F association, we designed the dodecapeptide Zwit-1F, which we crystallized to obtain the first high-resolution images of a 14-helical  $\beta$ -peptide bundle.<sup>6</sup> A detailed thermodynamic analysis established that the solution-phase behavior of Zwit-1F was consistent with an equilibrium between unfolded monomers and folded octamers with an association/folding constant of  $4 \times 10^{30} \text{ M}^{-7}$  at 25 °C.<sup>7</sup>

The Zwit-1F octamer contains four copies of a parallel  $\beta$ -peptide dimer. Each parallel dimer associates in an antiparallel fashion with another dimer to form a tetramer, and two tetramers assemble with a 39° crossing angle to form the octamer (Figure 1A). The octamer core is composed entirely of solvent-inaccessible  $\beta^3$ -homoleucine ( $\beta^3\text{L}$ ) residues; hydrophobic burial of their side chains presumably drives association. The solvent-exposed octamer surface is decorated by  $\beta^3$ -homoglutamate ( $\beta^3\text{E}$ ),  $\beta^3$ -homoaspartate ( $\beta^3\text{D}$ ), and  $\beta^3$ -homomethionine ( $\beta^3\text{O}$ ) residues that are charge-paired within the dimer unit and across the dimer/dimer or tetramer/tetramer interfaces.

While we regarded the crystal structure as an important step toward the design of a higher order  $\beta$ -peptide fold, several factors make Zwit-1F nonideal. First, it has a low self-affinity: the concentrations at which 50% ( $C_{50}$ ) or 90% ( $C_{90}$ ) of Zwit-1F exists in the folded, octameric state are 50 and 350  $\mu\text{M}$ , respectively. Second, because of the complete surface charge pairing and exclusively 14-helical structure, the Zwit-1F octamer contains no easily modified residues and no pocket to support ligand binding and catalysis. Last, the octameric stoichiometry complicates interpretation of self-association data and increases the chance that substitution of any single side chain will alter the Zwit-1F fold.

We considered two strategies to identify longer  $\beta$ -peptides that could recapitulate the Zwit-1F fold with fewer subunits (Figure 1A). One, which was not pursued, involves joining the antiparallel strands of a single tetramer with an appropriate (albeit lengthy) linker (Strategy A); the strategy reported here reverses the relative

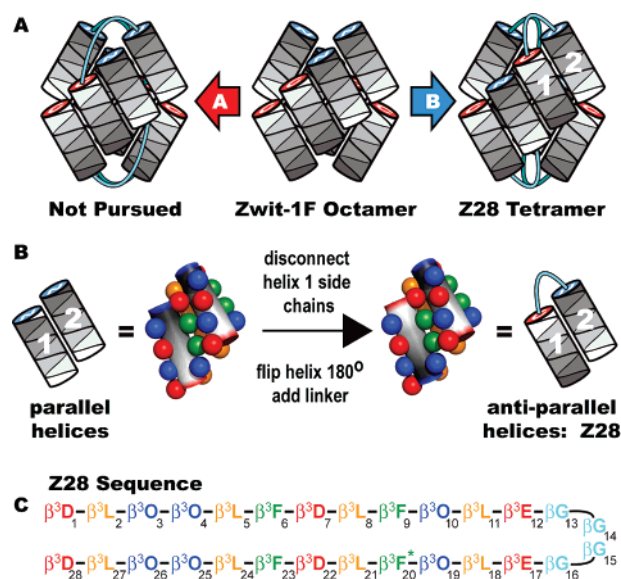


**Figure 1.** (A) Two strategies for conversion of the Zwit-1F octamer into a tetramer. (B) Details of Strategy B. We began with a parallel dimer unit (helices 1 and 2) from the Zwit-1F crystal structure and proceeded as described in the text. Sphere representations of side chains are colored by residue type as in the sequence. (C) Sequence of Z28.  $\beta$ -Amino acids are represented by the single letter code of the equivalent  $\alpha$ -amino acid. F\* denotes *p*-iodophenylalanine and O denotes ornithine.  $\beta\text{G}$  is commonly referred to as  $\beta$ -alanine.

orientation of the two internal  $\beta$ -peptide monomers, converting four copies of a noncovalent parallel dimer into four copies of a covalent antiparallel dimer, Z28 (Strategy B).

To reverse the relative orientation of the two internal  $\beta$ -peptides in each tetramer of Zwit-1F, we used Spartan<sup>8</sup> to convert each of the four parallel  $\beta$ -peptide dimers that comprise the octamer into an antiparallel dimer (Figure 1B). The side chains of the interior helix of each parallel dimer (helix 1) were disconnected, and the  $\beta$ -peptide backbone was flipped axially by 180°. The side chains were then reconnected and the backbone structure energy-minimized with the side chains fixed. The now antiparallel  $\beta$ -peptide dimers were then connected by  $\beta\text{G}$  linkers of varying lengths, and a four  $\beta\text{G}$  linker was determined to be the shortest that could span the two helices. Finally, the resulting 28 residue structure was energy-minimized. This modeling exercise suggested that the antiparallel helix-loop-helix structure, which we call Z28 (Figure 1C), could replace each parallel dimer unit in Zwit-1F, effectively placing the side chains in the same regions of space as the parallel dimer from Zwit-1F (Figure S1 in Supporting Information).

It has previously been shown that the purity of  $\beta$ -peptides prepared using solid-phase synthesis falls off precipitously with chain length.<sup>9,10</sup> We sought methods that could yield  $\beta$ -peptide 28-

<sup>†</sup> Department of Chemistry.

<sup>‡</sup> Department of Molecular, Cellular and Developmental Biology.

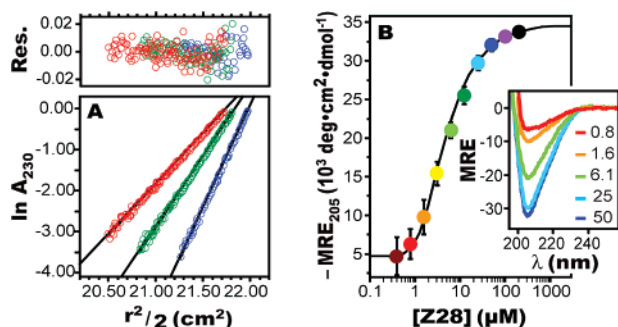


**Figure 2.** (A) AU sedimentation equilibrium at 42 kRPM (red), 50 kRPM (green), and 60 kRPM (blue) fit to a single ideal species of 14.8 kDa ( $n = 4.0$ ). Residuals are displayed with a linear  $Y$ -axis scale. (B) Z28 concentration-dependent CD data. The molar residue ellipticity at 205 nm ( $MRE_{205}$ ) fit to a monomer–tetramer equilibrium where  $MRE_{\text{mon}} = 4.7 \times 10^3 \text{ deg}\cdot\text{cm}^2\cdot\text{dmol}^{-1}$ ,  $MRE_{\text{tet}} = 34.8 \times 10^3 \text{ deg}\cdot\text{cm}^2\cdot\text{dmol}^{-1}$ , and  $\ln K_a = 37.5$ . Inset: Wavelength-dependent CD data at the indicated concentrations (in  $\mu\text{M}$ ). MRE in units of  $10^3 \text{ deg}\cdot\text{cm}^2\cdot\text{dmol}^{-1}$ . AU and CD measurements were performed in 10 mM phosphate, 200 mM NaCl (pH 7.2).

mers of high purity without need for large excesses of costly  $\beta$ -amino acid monomers. Z28 was first synthesized in the standard way, using a single coupling with 3 equivalents of Fmoc-protected  $\beta$ -amino acid monomer, HOBt, and PyBOP. Solutions of 20% piperidine (Pip) in DMF were used for Fmoc removal, and both coupling and deprotection steps were performed with microwave irradiation. Most short (7- to 12-mer)  $\beta$ -peptides synthesized this way are purified effectively by a single HPLC pass in yields of 20–40%.<sup>11</sup> This protocol failed for Z28: the desired product was contaminated by many peptidic side products (6% purity by LC area percentage, LCAP), so that we isolated Z28 in less than a 1% yield.

The synthesis and purity of Z28 were optimized in several steps. Significant improvements were observed upon inclusion of a second piperidine deprotection step and substitution of PyBOP and HOBt with PyAOP and HOAt (see Supporting Information).<sup>12</sup> Our final synthetic procedure used 3 equiv of  $\beta$ -amino acid, PyAOP, and HOAt; deprotections with one 20% piperidine treatment and two treatments with 2% DBU; and  $\text{Ac}_2\text{O}$  capping after every fourth amino acid. This procedure provided Z28 in 19% isolated yield at an LCAP purity of 42%, values that compare favorably with those generally seen for  $\beta$ -peptide 12-mers. Thus, we avoided having to use segment condensation reactions by optimizing microwave coupling conditions for the linear synthesis of Z28.

With sufficient quantities of Z28 in hand, we characterized its association and stability using analytical ultracentrifugation (AU), circular dichroism (CD) spectroscopy, 8-anilino-naphthalene sulfonate (ANS) binding,  $^1\text{H}$  NMR, and light scattering measurements. Consistent with our design, Z28 sedimented as an ideal tetramer upon ultracentrifugation, producing linear  $\ln(\text{absorbance}_{230\text{nm}})$  versus (radial distance)<sup>2</sup> plots at three speeds (Figure 2A).<sup>13</sup> Indeed, the observation that Z28 behaves as a single ideal species implies that it possesses higher self-affinity than Zwit-1F, which could be fit only as an equilibrating species. Moreover, the Z28 assembly is stable under a range of solution conditions—it sediments as a tetramer in Tris buffer at pH 8.5 or 10.0 and in phosphate buffer at pH 6.0 or 7.2. At pH 6.0, weak dimerization to form octamers occurs ( $C_{50} = 41 \mu\text{M}$ ,  $C_{90} = 1.9 \text{ mM}$ ), but no disintegration of the tetramer is observed.

Next, we used CD spectroscopy at concentrations from 0.39 to 200  $\mu\text{M}$  to evaluate the stability of the tetrameric Z28 fold (Figure 2B). The molar residue ellipticity at 205 nm ( $MRE_{205}$ ) of 200  $\mu\text{M}$  Z28 is  $-34\,820 \text{ deg}\cdot\text{cm}^2\cdot\text{dmol}^{-1}$ , 4 times the value measured for Zwit-1F at an equivalent oligomer concentration ( $-8700 \text{ deg}\cdot\text{cm}^2\cdot\text{dmol}^{-1}$  at 400  $\mu\text{M}$ ). The  $MRE_{205}$  concentration dependence fits well ( $R = 0.999$ ) to a monomer–tetramer equilibrium with an association

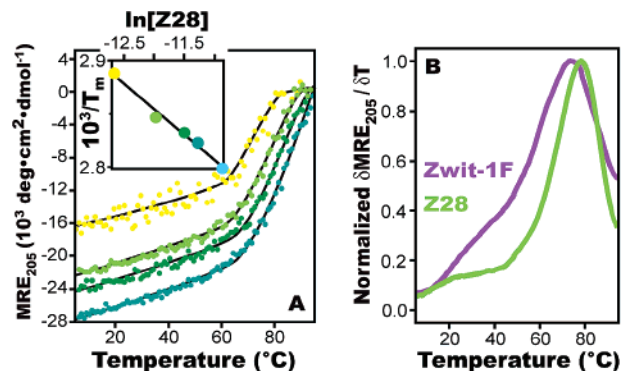


**Figure 3.** (A) Temperature dependence of the molar residue ellipticity at 205 nm ( $MRE_{205}$ ) of 3.125 (yellow), 6.25 (light green), 10.0 (dark green), and 12.5 (teal)  $\mu\text{M}$  Z28 in phosphate buffer (pH 7.2). Inset: Inverse thermal denaturation midpoints ( $1/T_m$ , in  $10^{-3} \text{ K}^{-1}$ ) at various concentrations of Z28 (3.125, 6.25, 10.0, 12.5, and 18.75  $\mu\text{M}$ ) fit to eq 1 as described in Supporting Information. (B) Normalized temperature derivatives of  $MRE_{205}$  for 150  $\mu\text{M}$  Zwit-1F and 6.25  $\mu\text{M}$  Z28.

constant of  $1.6 \times 10^{16} \text{ M}^{-3}$ . This value corresponds to a  $C_{50}$  of 4.7  $\mu\text{M}$  ( $C_{90} = 49 \mu\text{M}$ ), 10-fold lower than the  $C_{50}$  of Zwit-1F. The CD data are consistent with the AU data in that the concentrations observed in the AU cell range from 9 to 90  $\mu\text{M}$ , all of which should be at least 65% folded and tetrameric.

Temperature-dependent CD studies show Z28 to exhibit a concentration-dependent  $T_m$ , an inherent property of protein quaternary structure (Figure 3A). The Z28  $T_m$ , which increases from 73  $^{\circ}\text{C}$  at 3.125  $\mu\text{M}$  to roughly 92  $^{\circ}\text{C}$  at 31.25  $\mu\text{M}$ , is higher than the  $T_m$  of 100  $\mu\text{M}$  Zwit-1F (69  $^{\circ}\text{C}$ ). Roughly 25% of the CD signal is lost prior to cooperative unfolding of Z28, indicating flexibility in the folded structure. However, the width of the temperature derivative of the Z28 CD signal ( $\delta MRE_{205}/\delta T$ ) at half-maximum is 25 versus 40  $^{\circ}\text{C}$  for 150  $\mu\text{M}$  Zwit-1F, implying increased cooperativity in Z28 unfolding (Figure 3B).<sup>14</sup> Z28 unfolding is 92% reversible, as judged by recovery of the CD signal at 25  $^{\circ}\text{C}$  following thermal denaturation.<sup>15,16</sup>

The temperature-independent van't Hoff enthalpy ( $\Delta H_{\text{vH}}$ ) of a self-associating system can be determined from the slope of a plot of  $1/T_m$  versus  $\ln[Z_T]$ , where  $Z_T$  is the total concentration of monomer units (Figure 3A).<sup>14</sup> For Zwit-1F and Z28, this analysis yields  $\Delta H_{\text{vH}}$  values of 104 and 124  $\text{kcal}\cdot\text{mol}^{-1}$ , respectively (see Supporting Information). Thus, both concentration- and temperature-dependent CD analysis, as well as AU analysis, indicate that Z28 is substantially more stable than Zwit-1F. We note, however, that  $\Delta H_{\text{vH}}$  measurements must be treated with caution, as more thorough calorimetric analysis found the Zwit-1F enthalpy of denaturation to be temperature-dependent.<sup>7,17</sup>

We also characterized the Z28 fold by the extent to which it influenced ANS fluorescence and by  $^1\text{H}$  NMR. ANS increases in fluorescence when sequestered in a hydrophobic environment.<sup>18,19</sup> A protein-dependent increase in ANS fluorescence suggests that the protein core is sufficiently fluid to allow invasion by ANS. In the presence of 200  $\mu\text{M}$  Z28 (96% tetrameric), ANS fluorescence increased 12-fold over background in phosphate buffer at pH 7.2 (see Supporting Information). While direct comparison to Zwit-1F ANS binding is precluded by the fact that Zwit-1F forms insoluble aggregates in the presence of ANS, a 12-fold fluorescence increase is generally regarded as evidence of a molten hydrophobic core.<sup>20</sup> Additional evidence for the plasticity of the Z28 core was found in the  $^1\text{H}$  NMR spectrum (Figure S4 in Supporting Information). At 400  $\mu\text{M}$  in phosphate buffer, no discrete amide N–H resonances were observed, whereas 10 discrete peaks could be observed in

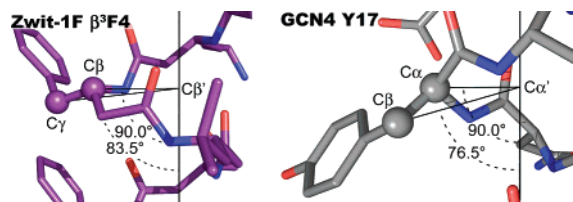


**Figure 4.** Left: The Zwit-1F side chain display angle, made by the  $\gamma$  carbon ( $C_\gamma$ ), the projection of the  $\beta$ -carbon on the helix axis ( $C\beta'$ ), and the C-terminus of the helical axis ( $C$ ). The  $C_\gamma$ ,  $C\beta'$ ,  $C$  angle is shown for reference. Right: The analogous  $C\beta$ ,  $C\alpha'$ ,  $N'$  side chain display angle and  $C\alpha$ ,  $C\alpha'$ ,  $N'$  reference angle for GCN4 ( $N'$  = helical axis N-terminus).

the Zwit-1F amide region at 750  $\mu$ M (95% folded). The higher affinity, more cooperative fold of Z28 appears to be related its topology, as the hydrophobic core is not as well packed as the Zwit-1F core.

In the absence of high-resolution structural characterization, sedimentation velocity AU and size-exclusion chromatography coupled light scattering (SEC-LS) experiments were used to show that the Z28 oligomer adopts a compact, nearly spherical fold ( $f/f_0 = 1.1$ ). The hydrodynamic radius ( $R_H = 19 \text{ \AA}$ ) measured by SEC-LS is consistent with the radius (20  $\text{\AA}$ ) of our computational model of the tetramer and not with an elongated fold (see Supporting Information for models, AU data, and SEC-LS data.)

Inherent in the design of Z28 is the assumption that the flipped helix—which is formally a “retro”  $\beta^3$ -peptide—will present its side chains in a manner that closely resembles the original  $\beta$ -peptide helices: analogous “retro” analogues of the GCN4 leucine zipper domain formed poorly folded mixtures or oligomers of different stoichiometries than their parent.<sup>21–23</sup> We propose that the design of Z28 succeeded because of two defining characteristics of the 14-helix: the linear arrangement of side chains along one helix face, a direct consequence of a 3.1 residue repeat, and the nearly flat trajectory of  $\beta$ -peptide side chains as they emerge from the helix axis. The side chains of Zwit-1F helix 1 on average project at 84.6° to the helical axis, a value significantly closer to 90° than the corresponding angle for a GCN4  $\alpha$ -helix (77.7°) (Figure 4 and Supporting Information). The small deviation of the 14-helix projection angle from 90° implies that helix flipping will minimally alter side chain display.

In summary, we successfully converted the parallel  $\beta$ -peptide dimer unit embodied in the octameric Zwit-1F  $\beta$ -peptide bundle into a linear, single chain 28 residue  $\beta$ -peptide. We optimized microwave-assisted synthesis conditions to enable a linear assembly of Z28 in sufficient yields and purity to make future analogue syntheses routine. Z28 is, to our knowledge, the longest  $\beta$ -peptide yet synthesized. CD and AU experiments indicate that Z28 is tetrameric as expected. Furthermore, the CD data show that Z28 unfolds more cooperatively than Zwit-1F, with a higher affinity

and a larger  $\Delta H_{\text{vH}}$ . Thus, we have overcome the problems associated with Zwit-1F: Z28 is a stable  $\beta$ -peptide bundle of reasonable stoichiometry with a region of  $\beta$ G residues that should be amenable to functionalization. Z28 is an important step toward protein-like  $\beta$ -peptides, and the apparent ease of flipping the 14-helical epitope may soon enable the design of even more complex geometries.

**Acknowledgment.** This work was supported by grants to A.S. from the NIH and the National Foundation for Cancer Research. E.J.P. thanks the NIH for fellowship support, and Dr. Foltast-Stogniew of the Keck Foundation Biotechnology Resource Laboratory at Yale University for assistance with SEC-LS.

**Supporting Information Available:** Descriptions of the synthesis of Z28 and its characterization by MS/MS sequencing, AU, CD, ANS fluorescence,  $^1\text{H}$  NMR, and SEC-LS, as well as analysis of the side chain display angles of Zwit-1F and GCN4 are provided in Supporting Information. This material is available free of charge via the Internet at <http://pubs.acs.org>.

## References

- (1) Anfinsen, C. B. *Science* **1973**, *181*, 223–230.
- (2) Bryson, J. W.; Betz, S. F.; Lu, H. S.; Suich, D. J.; Zhou, H. X. X.; Oneil, K. T.; Degrad, W. F. *Science* **1995**, *270*, 935–941.
- (3) Goodman, C. M.; Choi, S.; Shandler, S.; DeGrado, W. F. *Nat. Chem. Biol.* **2007**, *3*, 252–262.
- (4) Benner, S. A.; Sismour, A. M. *Nat. Rev. Genet.* **2005**, *6*, 533–543.
- (5) Qiu, X. J.; Petersson, E. J.; Mathews, E. E.; Schepartz, A. *J. Am. Chem. Soc.* **2006**, *128*, 11338–11339.
- (6) Daniels, D. S.; Petersson, E. J.; Qiu, X. J.; Schepartz, A. *J. Am. Chem. Soc.* **2007**, *129*, 1532–1533.
- (7) Petersson, E. J.; Craig, C. J.; Daniels, D. S.; Qiu, X. J.; Schepartz, A. *J. Am. Chem. Soc.* **2007**, *129*, 5344–5345.
- (8) *Spartan '04*; Wavefunction, Inc.: Irvine, CA.
- (9) Abele, S.; Guichard, G.; Seebach, D. *Helv. Chim. Acta* **1998**, *81*, 2141–2156.
- (10) Seebach, D.; Abele, S.; Sifferlen, T.; Hanggi, M.; Gruner, S.; Seiler, P. *Helv. Chim. Acta* **1998**, *81*, 2218–2243.
- (11) Murray, J. K.; Gellman, S. H. *Org. Lett.* **2005**, *7*, 1517–1520.
- (12) Albericio, F.; Cases, M.; Alsina, J.; Triolo, S. A.; Carpino, L. A.; Kates, S. A. *Tetrahedron Lett.* **1997**, *38*, 4853–4856.
- (13) Laue, T. M. Sedimentation equilibrium as thermodynamic tool. In *Methods in Enzymology: Energetics of Biological Macromolecules*; Academic Press: New York, 1995; Vol. 259, pp 427–452.
- (14) Marky, L. A.; Breslauer, K. J. *Biopolymers* **1987**, *26*, 1601–1620.
- (15) Sturtevant, J. M. *Annu. Rev. Phys. Chem.* **1987**, *38*, 463–488.
- (16) Although an ideal two-state transition exhibits 100% reversibility, the thermal denaturation of many natural proteins has been interpreted in terms of a two-state model despite reversibilities as low as 80%. See, for example: Hible, G.; Renault, L.; Schaeffer, F.; Christova, P.; Radulescu, A. Z.; Evrin, C.; Gilles, A. M.; Cherfils, J. *J. Mol. Biol.* **2005**, *352*, 1044–1059.
- (17) Kaya, H.; Chan, H. S. *Proteins: Struct. Funct. Bioinf.* **2000**, *40*, 637–661.
- (18) Goto, Y.; Fink, A. L. *Biochemistry* **1989**, *28*, 945–952.
- (19) Semisotnov, G. V.; Rodionova, N. A.; Razgulyaev, O. I.; Uversky, V. N.; Gripas, A. F.; Gilmanshin, R. I. *Biopolymers* **1991**, *31*, 119–128.
- (20) Lumb, K. J.; Kim, P. S. *Biochemistry* **1995**, *34*, 8642–8648.
- (21) Mittl, P. R. E.; Deillon, C.; Sargent, D.; Liu, N. K.; Klausner, S.; Thomas, R. M.; Gutte, B.; Grutter, M. G. *Proc. Natl. Acad. Sci. U.S.A.* **2000**, *97*, 2562–2566.
- (22) Liu, N. K.; Deillon, C.; Klausner, S.; Gutte, B.; Thomas, R. M. *Protein Sci.* **1998**, *7*, 1214–1220.
- (23) Holtzer, M. E.; Braswell, E.; Angeletti, R. H.; Mints, L.; Zhu, D.; Holtzer, A. *Biophys. J.* **2000**, *78*, 2037–2048.

JA077245X